Article citation info:
Zadrąg R, Socik P, Kniaziewicz T, Zacharewicz M, Bogdanowicz A, Wirkowski P. Analysis of simulated dynamic loads of a ship propulsion system of a non-conventional power system. Combustion Engines. 0000;XXX(X):xx-xx. https://doi.org/10.19206/CE-184139

Ryszard ZADRĄG
Paweł SOCIK
Tomasz KNIAZIEWICZ
Marcin ZACHAREWICZ
Artur BOGDANOWICZ
Paweł WIRKOWSKI

Combustion Engines
Polish Scientific Society of Combustion Engines

Analysis of simulated dynamic loads of a ship propulsion system of a non-conventional power system

ARTICLE INFO

Received: 24 November 2023
Revised: 12 February 2024
Accepted: 15 February 2024
Available online: 7 March 2024

Unconventional approaches to propulsion system design are increasingly being explored to meet increasing demands for efficiency, ecology, and reliability. This paper focuses on the analysis of simulated dynamic loads on the propulsion system of ships that feature unconventional power systems – Reformed Methanol Fuel Cell System (RMFC). The analysis is aimed at understanding the performance of these systems under dynamic sea conditions, assessing their performance, and identifying potential challenges and benefits associated with them (including military ones). According to military assumptions, an undeniable benefit is the minimization of the ship's physical fields and its independence from the base (i.e., in the future, obtaining hydrogen from seawater electrolysis).

Key words: *marine diesel combustion engine, RMFC, fuel cell, methanol reforming, hydrogen*

1. Introduction

Today's marine technology is constantly evolving, striving for ever more advanced and efficient solutions. One of the core components of modern vessels is their propulsion system, which plays a key role in ensuring not only efficiency but also the sustainability of the marine environment. Increasingly, unconventional approaches to propulsion system design are being explored to meet the growing demands for efficiency, ecology, and reliability.

In addition to the aforementioned commercial requirements, special – purpose entities – such as the military – focus additionally on logistical aspects (independence from the base), and stealthiness of operations (minimizing the physical ship, including acoustic and thermal). These aspects can be provided by propulsion systems equipped with hydrogen-powered fuel cells.

The conditions of use of marine main propulsion engines are peculiar, resulting from the resistance characteristics of the vessel and the characteristics of the propellers. The movement of the vessel is characterized by significant dynamics resulting from changes in the external conditions of swimming, which significantly affects the course of the resistance characteristics and, thus, changes in the power of the main engines at a given speed of swimming. The dynamic change of loads, during which there is a change in the performance of the propulsion system at a given time, occurs as a result of steering, the interaction of external conditions as well as their correlation. Typical dynamic conditions occur during starting from a standstill, changes in speed, changes in the direction of movement of the vessel, sailing in storm conditions, working on DP, performing special tasks (e.g. fishing, trawling, searching for mines) [17].

Reciprocating internal combustion engines were the traditional solution adopted for most ships of the last century. The emerging sense of environmental responsibility in the early 20th century [15, 35] as the changing climate led to a change of approach in ship propulsion design [1]. The shipbuilding industry focused its efforts on implementing exhaust gas cleaning systems to ensure compliance with MARPOL regulations [3, 16]. The 21st century brought further restrictions on toxic exhaust emissions [16, 22], forcing the introduction of alternatives for energy efficiency as well as emission reduction.

Leo et al. [19] took up the study of PEM fuel cells in terms of exergy loss and exergy efficiency. He performed the analysis for PEM fuel cells powered by hydrogen produced by methanol reforming and direct methanol fuel cells powered by direct liquid methanol [19].

The issue of using hydrogen as an alternative power source at sea was dealt with, among others, by Meryem Gizem Sürer and Hüseyin Turan Arat. They summarized the latest research, hydrogen production, and storage methods and challenges, which allowed them to analyze the development of fuel cell-based marine vehicles [26].

Zuhang et al. [10] in their research present a literature analysis of the economics, feasibility, and primacy of fuel cells and hydrogen for marine applications in four aspects: key technologies for marine fuel cell applications, key technologies for marine hydrogen applications, costs, and standards.

Elammas [7] paper analyzed the environmental benefits of hydrogen fuel cells, including their potential to reduce greenhouse gas emissions and improve energy efficiency. In addition, he addressed the issues of improving energy security and reducing dependence on fossil fuels in maritime transportation.

One variant of the solution is the use of hybrid propulsion systems (HPS), which use electric motors, power generation systems, and power storage systems (Fig. 1). The downside of hybrid solutions is the increased weight of the vessel. However, the benefits of such a solution, including the high efficiency of the electric engine and the reduction of toxic exhaust emissions, outweigh the potential losses.

Satisfactory results obtained for hybrid propulsion systems encourage total propulsion electrification. An issue still being worked out is the optimization of electricity storage in batteries, the efficiency of this process depending on the speed and temperature of battery operation, and the thread of electricity production [2, 25, 32].

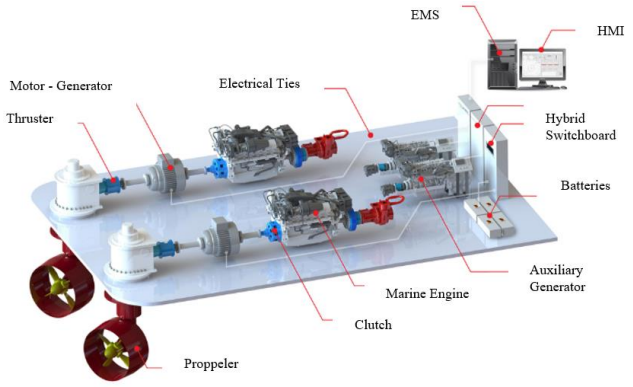

Fig. 1. AKA Hybrid propulsion [36]

A major trend in the development of marine propulsion systems is the use of alternative fuels such as hydrogen and its compounds. The revolution, which is already underway, is being driven by fuel cell (FC) technology and hybrid energy storage systems (HESS). Fuel cells are a quiet and clean energy source. On the plus side, fuel cells have a much higher energy density and high energy efficiency than batteries. Given these advantages, fuel cells themselves as well as hybrid systems have a promising future in marine applications [21, 22, 23]. One example of a hybrid system is the use of a PEMFC cell in a propulsion system in which an electrochemical battery can be recharged from a fuel cell (Fig. 2).

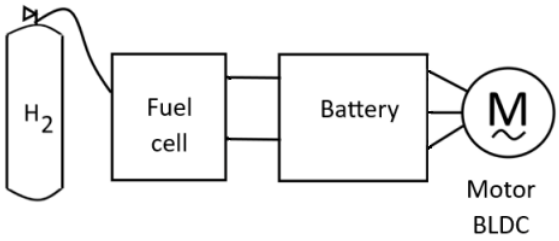

Fig. 2. Schematic of the construction ship propulsion system in which electrochemical battery can be recharged from a PEMFC

Among the 6 main types of fuel cells available (Table 1), which are used commercially, FCs containing a solid electrolyte are the most predisposed for power unit applications.

This group includes proton exchange polymer membrane fuel cells (PEMFCs), which can operate in the temperature range from 20 to 70°C (LT-PEMFC), and solutions operating at temperatures of 120–160°C (HT-PEMFC) [4, 31]. It should be noted that LT-PEMFC polymer cells, with respect to HT-PEMFCs, have already been used commercially in transportation for many years [5, 6, 31].

Despite the main advantage of LT-PEMFCs being low-temperature operation, they have one key disadvantage. In the use of these cells is the need to use high-purity hydrogen H2 (5N), due to the presence of a platinum catalyst. An example of an LT-PEMFC fuel cell stack is shown in Fig. 3. Unfortunately, the cost of the Pt catalyst, accounts for about 50% of the total cost of a PEMFC fuel cell stack. In addition, the Pt catalyst, shows very poor resistance to CO, SO_x (the possibility of catalyst degradation, leading to significant degradation of the electrical performance of the FC stack) [5, 6, 33].

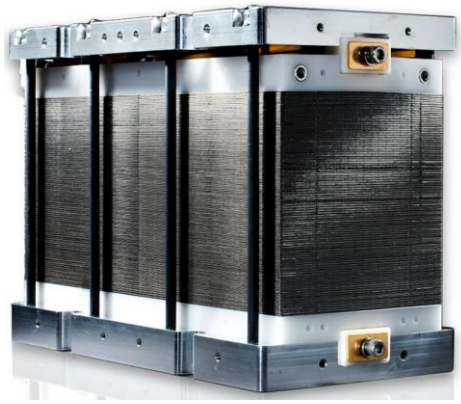

Fig. 3. Example PEM fuel cell stack [11]

LT-PEMFC fuel cells can operate as electricity generators in a wide range of electrical outputs from a few watts to several hundred kW. In turn, these units can be combined in a modular fashion (i.e., series connection of smaller units, parallel connection of more units) or electrically connected in series-parallel to form high-power generators, i.e., the 15–19 MW range [5, 6].

Table 1. Types of fuel cells [9, 31]

Type of cell	Electrolyte	Operating temperature [°C]	Fuel	Efficiency [~%]	Application
PEMFC – polymer membrane fuel cell	solid polymer	20–160	H_2, N_2H_4, CH_4 – fuel and oxidizer devoid of CO_2	53–58	astronautics, military technology
AFC – alkaline fuel cell	solution KOH	50–200	H_2, N_2H_4, CH_4	60	astronautics, military technology
DMFC – methanol fuel cell	solid polymer	20–90	methanol	40	portable
PAFC – phosphoric acid fuel cell	Concentrated H_3PO_4	150–200	H_2, CH_3OH, natural gas, kerosene, biogas	> 40	public facilities
MCFC – molten carbonate fuel cell	fused carbonate (Li, K, Na)	600–700	CH_3OH, natural gas, biogas	45	power generation
SOFC – solid oxide fuel cell	ZrO_2:$Y2O_3$	500–1000	H_2, CH_4, natural gas, biogas	35–43	power engineering, cogeneration

PEMFC generators have an electrical efficiency of 45–65%,The rest of the energy is lost as heat. In order to remove heat from the fuel cell space, they must have cooling systems. Liquid cooling systems are used at scales above 10 kW. It should be noted that the heat from LT-PEMFC fuel cells can be recovered and used in the system, raising the efficiency of the integrated energy system to 70–80% [8, 28].

As a rule of thumb, LT-PEMFC fuel cells require a supply of 0.8 m^3 of H_2 (at 50% efficiency) to produce 1 kWh. Based on this relationship, it can be assumed that an FC generator (FC stack module of 100 kW, to produce 100 kWh will require the supply of 80 m^3 of H_2 or 7.12 kg of H_2. In the case of FC LT-PEMFC generators, it is necessary to take into account about 2–3% H_2 of hydrogen additionally for the so-called own needs (purification, membranes, over–blowing). Media outlet temperatures from the media cooling system and from the cathode space are in the range of 45–55^{o}C [6, 15, 24, 34].

This article focuses on analyzing the simulated dynamic loads of a ship's propulsion system, which features an unconventional power system (in this case, a power generation module consisting of a 5 kW fuel cell powered by reformer-generated hydrogen (RMFC)). The analysis of such a solution is aimed at understanding their performance under dynamic maritime conditions, assessing their performance, and identifying possible challenges and benefits associated with them.

The conclusions of this analysis may have important implications for the future of marine transportation and vessel operations. By considering unconventional power systems, we are able to chart development paths that will contribute to a more sustainable and efficient use of marine resources, while reducing environmental impact.

In terms of military application, the key is to achieve independence from fossil fuels, which, during a potential conflict, can increase the operational potential of the ships. In addition, which is also part of the research issue, the use of RMFCs allows for minimizing the ship's thermal field by lowering the temperature of the exhaust gases.

2. Research object

In order to carry out the study, it was necessary to obtain the actual load spectra of the marine engine. Data were obtained from a vessel equipped with an MTU 8V2000 M72 propulsion engine (Fig. 4).

Fig. 4. View of the MTU 8V2000 M72 engine [27]

Basic technical engine data is shown below in Table 2.

Table 2. Technical data of the MTU 8V2000 M72 engine [27]

Rated speed	rpm	2250
Rated power	kW	720
Number of cylinders	–	8
Cylinder arrangement and quantity	^{o}	90
Piston stroke	mm	156
Cylinder diameter	mm	135
Cylinder displacement	cm^3	2230
Total engine displacement	cm^3	17840
Number of inlet valves per cylinder	–	2
Number of exhaust valves per cylinder	–	2

The object of laboratory research was a stationary test stand for power generation, which is located at the equipment of the Poznan University of Technology (Fig. 5). The configuration of this station allows simulation studies that faithfully, assuming the scalability of the processes, reflect the nature of load changes in the ship's propulsion system.

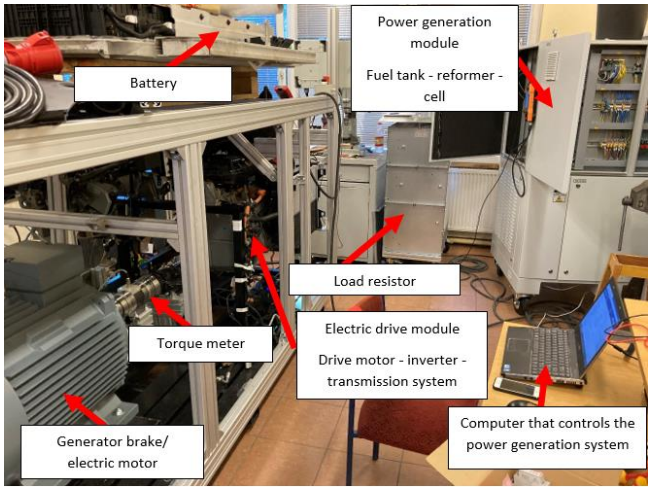

Fig. 5. Reformer test stand including battery, electric motor, power take-off system and data acquisition station

The main components of the stand (Table 3) are a power generation module (H3–5000 is a Reformed Methanol Fuel Cell System (RMFC)) consisting of a 5 kW fuel cell (HTPEM) powered by hydrogen generated in the reformer. The reformer, on the other hand, is powered by an aqueous methanol solution with a methanol–water ratio of 60/40. The stand also includes a battery, an electric motor and a resistor.

The operation of the test stand load system is controlled by software dedicated to the developed test stand design. The reformer feeding the fuel cell operated in automatic mode, selecting the fuel dose according to the charging current. The control interface is shown below (Fig. 6). To test toxic compounds, a TESTO 350 analyzer was used, which was plugged into the reformer's exhaust outlet.

Table 3. Technical specifications test bench [30]

RMFC		
Maximum power output	W	5000
Input/Output voltage	W	42/57
Output current	A	125
Fuel consumption	dm^3/kWh	0.9
Battery		
Total energy capacity	kWh	25.92
Operational energy capacity	kWh	23.30
Number of cells	–	192
Rated voltage of a single cell	V	3.75
Rated capacity of a single cell	Ah	36
Rated voltage	V	395
Electric motor		
Engine power	kW	65 at 3000 rpm
Continuous engine power	kW	43
Maximum torque	Nm	220 in the shaft speed range of 250–2500 rpm

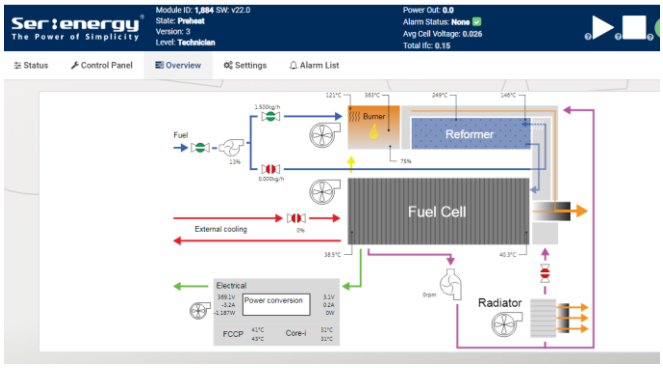

Fig. 6. RMCF data acquisition workstation interface

3. Research plan

In accordance with the research methodology, a research plan was developed, taking into account the research object, the measurement apparatus used and the measured parameters of the research object. Due to the complexity of the processes occurring during the load changes of the marine engine, it was decided to carry out tests for 4 cases determined on the basis of data collected on the vessel according to:

– the experimental plan of PS/DK 3^2
– the propeller characteristics
– the load histogram
– the battery charging plan.

Crankshaft speed, engine torque load, fuel consumption, exhaust toxic content and temperature, battery discharge/charge current, battery voltage, battery charge level were measured for the test object.

3.1. Research according to the experimental plan of PS/DK 3^2

Design of experiment (DoE) is often used to create empirical models. It reduces the number of measurements required, which translates into a reduction in the use of the object under study and, consequently, a reduction in costs. A properly selected research plan gives the possibility of obtaining accurate results, i.e., mathematical relationships describing selected process quantities [12 13, 20].

The study was planned using a static determined complete research plan (PS/DK 3^2), with which the influence of two input factors (crankshaft speed and engine torque load) was analyzed.

One of the steps in planning the experiment is to determine a set of characteristic quantities for the test object (Fig. 7), which were selected by introducing the following simplifications:

1. Constant values, due to their invariable influence on the waveform output values, are not taken into account
2. Interference factors are ignored due to studies conducted under identical environmental conditions
3 The set of input (independent) quantities is defined as follows:
   – shaft speed n = 300–1200 rpm
   – torque set on brake M = 0–60 Nm
4. The output quantities are limited to the quantities:
   – receiver (motor) power P [kW]
   – battery voltage U [V]
   – battery voltage drop dU [V/s]
   – battery current I_{bat} [A]
   – charging current I_{lad} [A]
   – battery charge level [%]
   – exhaust gas temperature t_{sp} [°C]
   – nitrogen oxides concentration in the exhaust gas NO_x [ppm]
   – nitrogen oxide concentration in the exhaust gas NO [ppm]
   – nitrogen dioxide concentration in the exhaust gas NO_2 [ppm]
   – carbon monoxide concentration in the exhaust gas CO [ppm]
   – carbon dioxide concentration in the exhaust gas CO_2 [%].

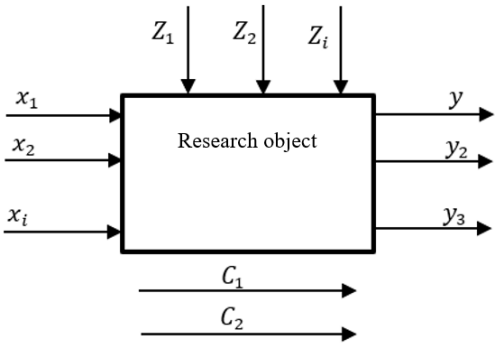

Fig. 7. Research object – structure. x – input quantities, y – output quantities, Z – disturbing quantities, C – constant values [37]

The values of the input parameters (in the number k) in the given intervals took over three levels of variation, which allows us to obtain a mathematical model of the studied process in the form of a polynomial of the second degree [37]:

$$y = b_0 + \sum b_k x_k + \sum b_{kk} x_k^2 + \sum b_{kj} x_k x_j \quad (1)$$

where: y – dependent output factor, x – j-th independent input factor, b – regression function coefficient.

The experiment was carried out according to the appropriate (for the chosen research plan) set of process input parameter values (Table 4).

Table 4. The experimental plan

Test	A	B	n [rpm]	M [Nm]
1	–1	–1	300	20
2	0	–1	750	20
3	1	–1	1200	20
4	–1	0	300	40
5	0	0	750	40
6	1	0	1200	40
7	–1	1	300	60
8	0	1	750	60
9	1	1	1200	60

The researcher were able to perform as few as nine tests, which made it possible to satisfactorily analyze the results obtained. In this plan:

- A is crankshaft rotational speed
- B is torque set on brake.

Number –1, 0 and 1 means lowest, middle and highest value of parameters A and B.

3.2. Research by propeller characteristics

The analysis by propeller characteristics was performed on the basis of the quantities obtained from the field of the MTU 8V2000 M72 engine (Fig. 8).

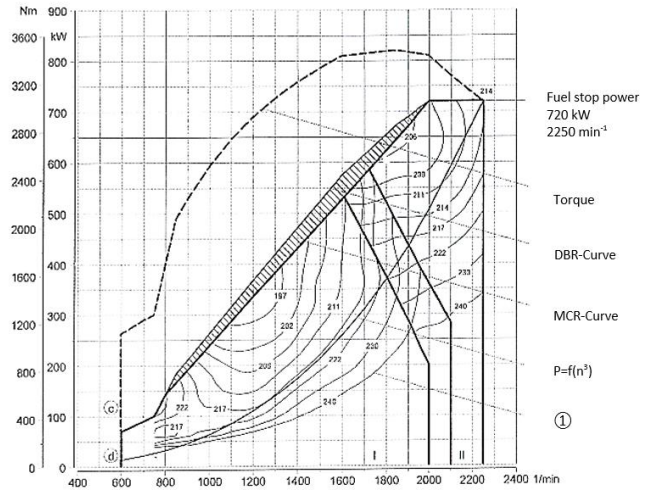

Fig. 8. MTU 8V2000 M72 engine work field. DBR – temporary work curve, WMT – maximum continuous work curve, P = f (n^3) – propeller characteristics, 1 – unit fuel consumption curves [27]

In order to perform the experiment, the assumed values of power and speed obtained from the working field were converted to denominated values to perform the bench test (Table 5).

Table 5. Independent parameter assumptions for the helical characteristics

No.	n [rpm]	M [Nm]	n/n_e	P/P_e	n [rpm]	M [Nm]
1	600	20	0.33	0.03	400	1.8
2	800	40	0.44	0.11	530	6.6
3	1000	60	0.55	0.16	660	9.6
4	1200	110	0.66	0.3	790	18
5	1400	170	0.77	0.46	920	27.6
6	1600	260	0.88	0.7	1050	42
7	1800	370	1	1	1200	60
	SHIP				TEST STAND	

3.3. Research according to the load diagram

Data from the ship's machine log was used to develop the load diagram. In the ship's machine log, load status information is recorded in the form of changes in engine speed. Records are made every hour of continuous operation or when the engine speed changes. Nowadays, this process is done automatically with the help of dedicated ship engine room monitoring programs.

Engine load processes during operation can be treated as a stochastic process (with engine standstill treated as an additional operating state) described by a process state space:

$$\Omega = \{e_1, e_2, e_3, e_4, e_5, e_6\} \quad (2)$$

where: e_1 – the operating condition of the engine in "loose gear", n = 600 rpm, e_2 – engine running condition on "very slow forward", n = 600 rpm, P_e = 0.03 P_z (20 kW), e_3 – engine running condition on "slow forward", n = 1200 rpm, P_e = 0.15 P_z (110 kW), e_4 – engine running condition at "half ahead", n = 1800 rpm, P_e = 0.51 P_z (370 kW), e_5 – engine running condition at "full ahead", n = 2250 rpm, P_e = P_z (720 kW), e_6 – „stop".

The power values for individual engine loads were determined indicatively for the ship's averaged propeller characteristics and assuming that in the ship's propulsion system the engines reach their rated operating point, i.e. for full displacement at rated speed value n = 2250 rpm the engines reach rated power P_z = 720 kW.

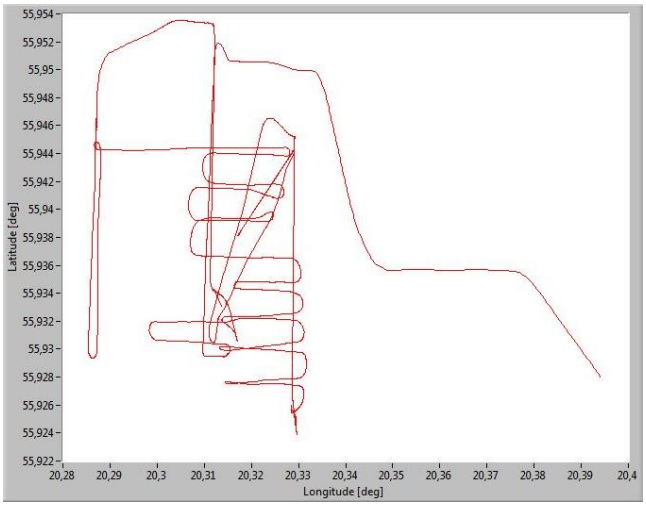

Fig. 9. The recorded path during the task searching by lanes

Also key to the operation of the ship's propulsion system is the type of task being performed, e.g. (minesweeping, patrolling, searching, identification). Each of the tasks requires different engine settings and introduces additional variables (e.g., changes in the direction of swimming, wind influence, making turns). An example of the path of a special–purpose vessel while performing a strip search task is shown in Fig. 9. Data for the chart was obtained from the "Automatic Identification System" AIS system.

Based on the values from the machine log, a histogram was developed for each working conditions (Fig. 10).

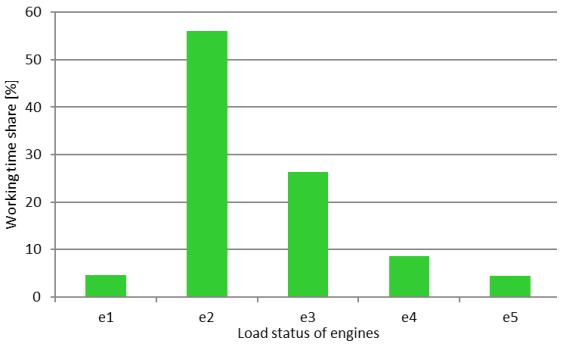

Fig. 10. Histogram of engines running time

In order to perform the experiment, the assumed values of power and speed obtained from the time balance of the motors (load histogram) were converted to denominated values, which allowed to perform the test on the test bench (Table 6).

Table 6. Independent parameter assumptions for the load diagram

Propulsion mode		n [rpm]	Usable power	Power for the propulsion mode [kW]	n [rpm]	M [Nm]
e1	luz	600	0	0	400	0
e2	BWN	600	P = 0.03 P_{max}	20	400	1.8
e3	WN	1200	P = 0.15 P_{max}	110	790	18
e4	PN	1800	P = 0.51 P_{max}	370	1200	60
e5	CN	2250	P = 1.0 P_{max}	720	1400	110
SHIP					TEST STAND	

3.4. Research according to the plan charging the battery

The analysis according to the 'battery charging' plan was carried out during battery charging using the system presented in Chapter 2. During start-up and preheating and cooling of the reformer, the test quantities were not measured due to the lack of measurement capabilities. Attention should be paid to the preparation time of the reformer for operation, i.e. the preheating process, which takes about 36 minutes, and the cooling time – 24 minutes. This accounts for about 33% of the device's operating time. The test plan for battery charging is shown in Table 7.

Table 7. The experimental plan for battery charging

No.	Battery charging current [A]	Measurement time [min]
–	start + preheating	36
–		
1	2	8
2	4	23
3	6	7
4	8	10
5	10	8
6	12	10
7	13	12
8	6	37
–	cooling + stop	24
–		

4. Test results

In accordance with the established test plan, all the mentioned parameters of engine operation were measured and recorded for the set speed, torque, and battery charging current. After the tests were performed, the obtained output values were analyzed in the STATISTICA program.

4.1. Analysis of the results for the experiment plan PS/DK 3^2

The analysis began by determining the significance of the influence of individual input parameters and their interactions were determined using ANOVA analysis of variance. The next step was to determine the quality of fit of the obtained (quadratic) models to the measured values was determined on the basis of coefficients of determination R^2 and standard deviation of the residual component s [12, 18, 29].

a)

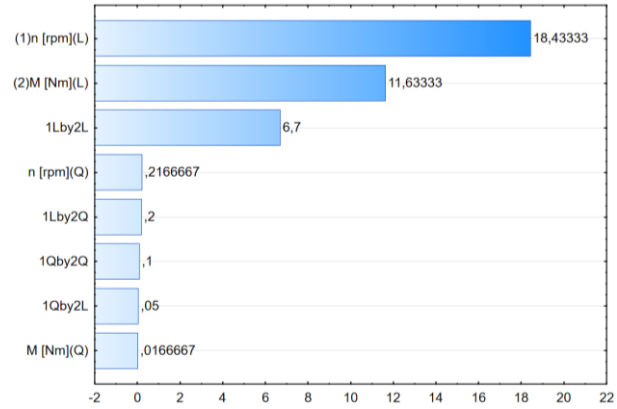

b)

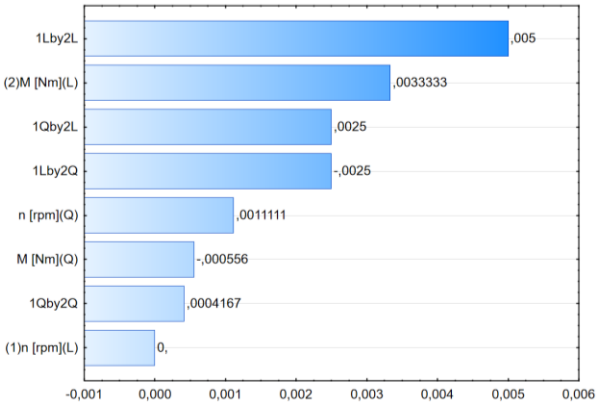

Fig. 11. Pareto charts of concentration of a) battery current I_{bat}, b) battery voltage drop dU

The approximated polynomials (1) allowed the determination of relationships between the variables, including the calculation and evaluation of the effect of loadings on the determination of correlations. Pareto charts were used for preliminary analysis.

Figure 11 shows the effect of individual independent factors and their interactions on battery performance indicators. The input quantities are represented on the vertical axis of the graph. Number 1 is crankshaft rotational speed, 2 – torque on the brake. The designation "L" means that the value of the coefficient is assigned to the linear magnitude of the polynomial, "Q" – to the quadratic magnitude, while "wz" – in relation to. As you can see, the main effect on the studied quantities is directly influenced by the speed as well as the torque, and for changes in battery voltage the relationship between the independent variables.

Based on the data obtained, surface plots were created and the changes in the parameters studied were presented as a function of fuel crankshaft speed and torque set on the brake (Fig. 12).

In the studied range of load and speed, the battery voltage drop was found to be the smallest for high loads and low speeds at the same time, or low loads and high speeds. The other studied parameters, such as power, battery discharge current, and battery charge level, show changes as expected, i.e., as the independent parameters increase, the values of battery current and receiver power increase, while the battery charge level decreases.

4.2. Analysis of results for propeller characteristics

For the results obtained, a slight spike in the battery charge value is visible (Fig. 13). This is due to both the time of measurement, which for technical reasons was limited to two minutes, and the small load variances of the system.

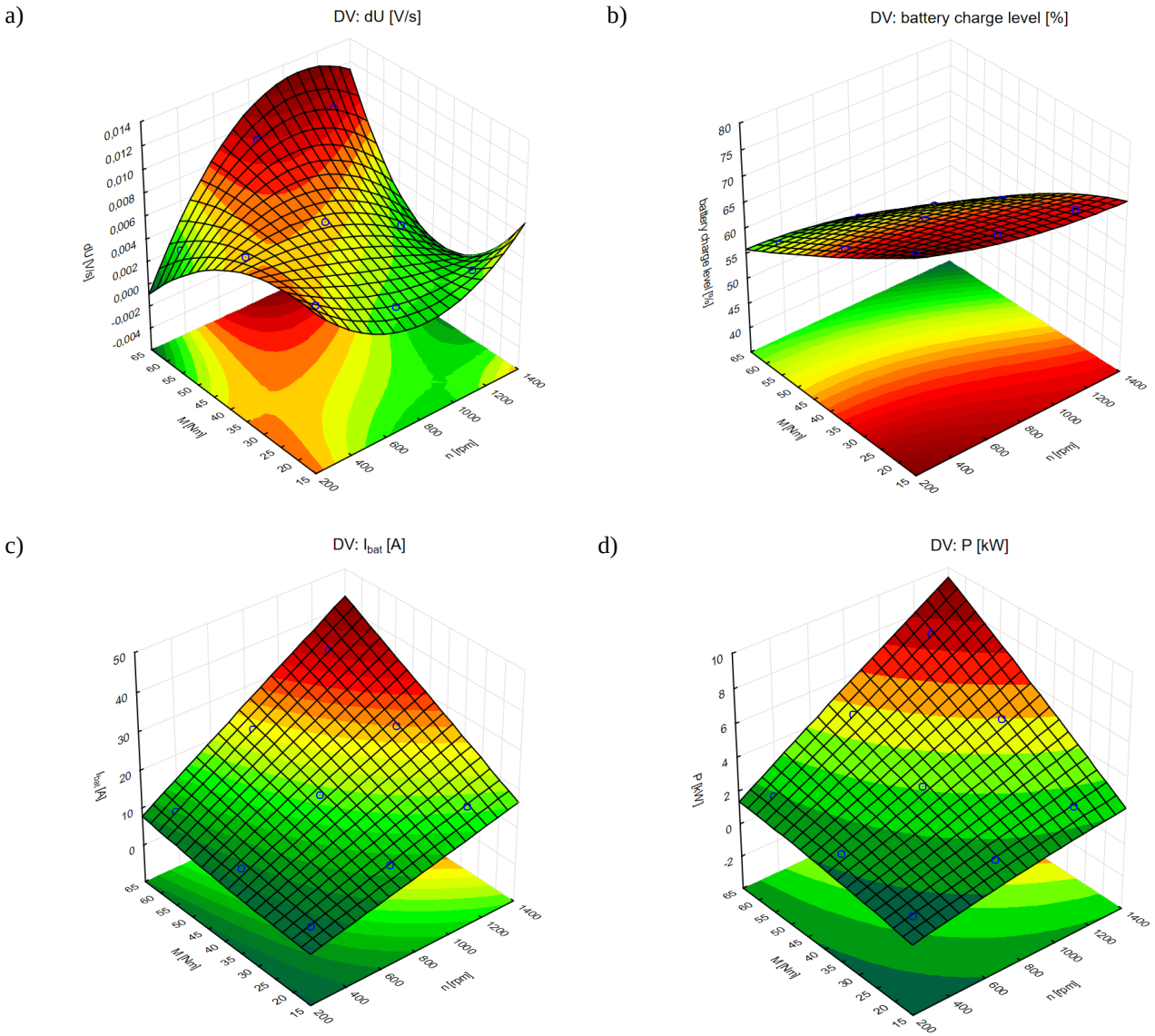

Fig. 12. Dependence of a) battery voltage drop, b) battery charge level, c) battery current, d) receive power

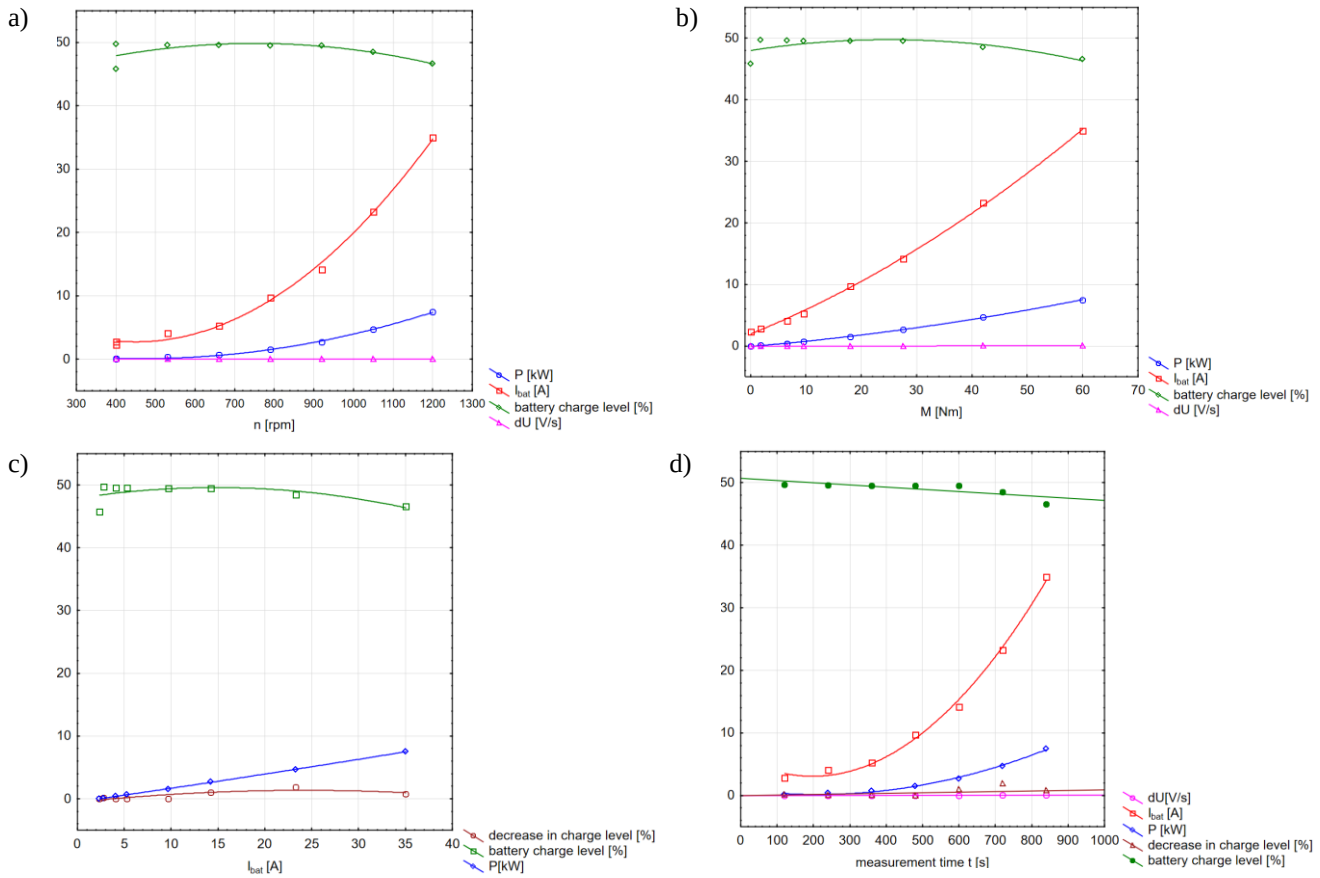

Fig. 13. Scatterplot of multiple variables against a) crankshaft rotational speed n, b) torque on the brake M, c) battery current, d) measurement time

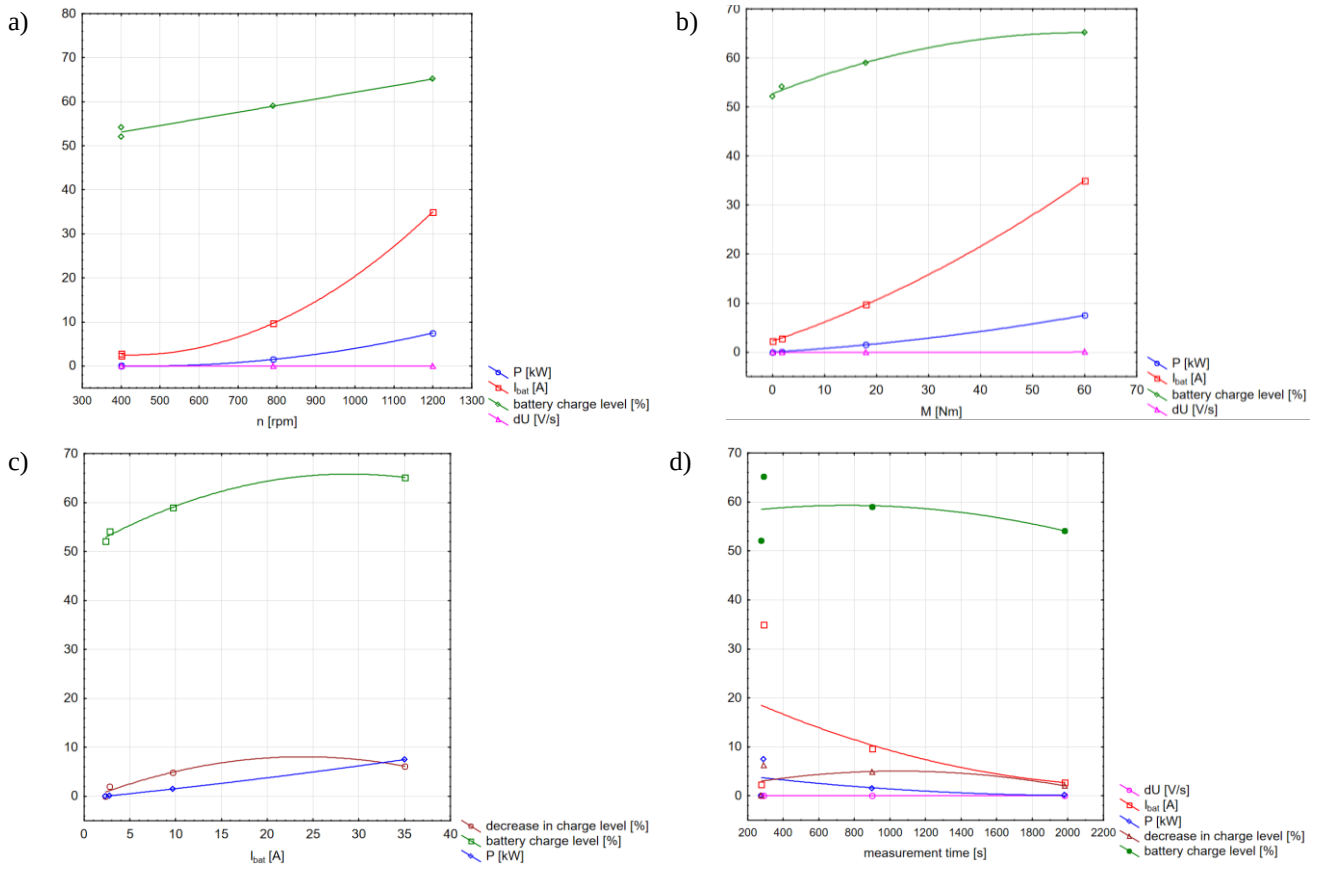

Fig. 14. Scatterplot of multiple variables against a) crankshaft rotational speed n, b) torque on the brake M, c) battery current, d) measurement time

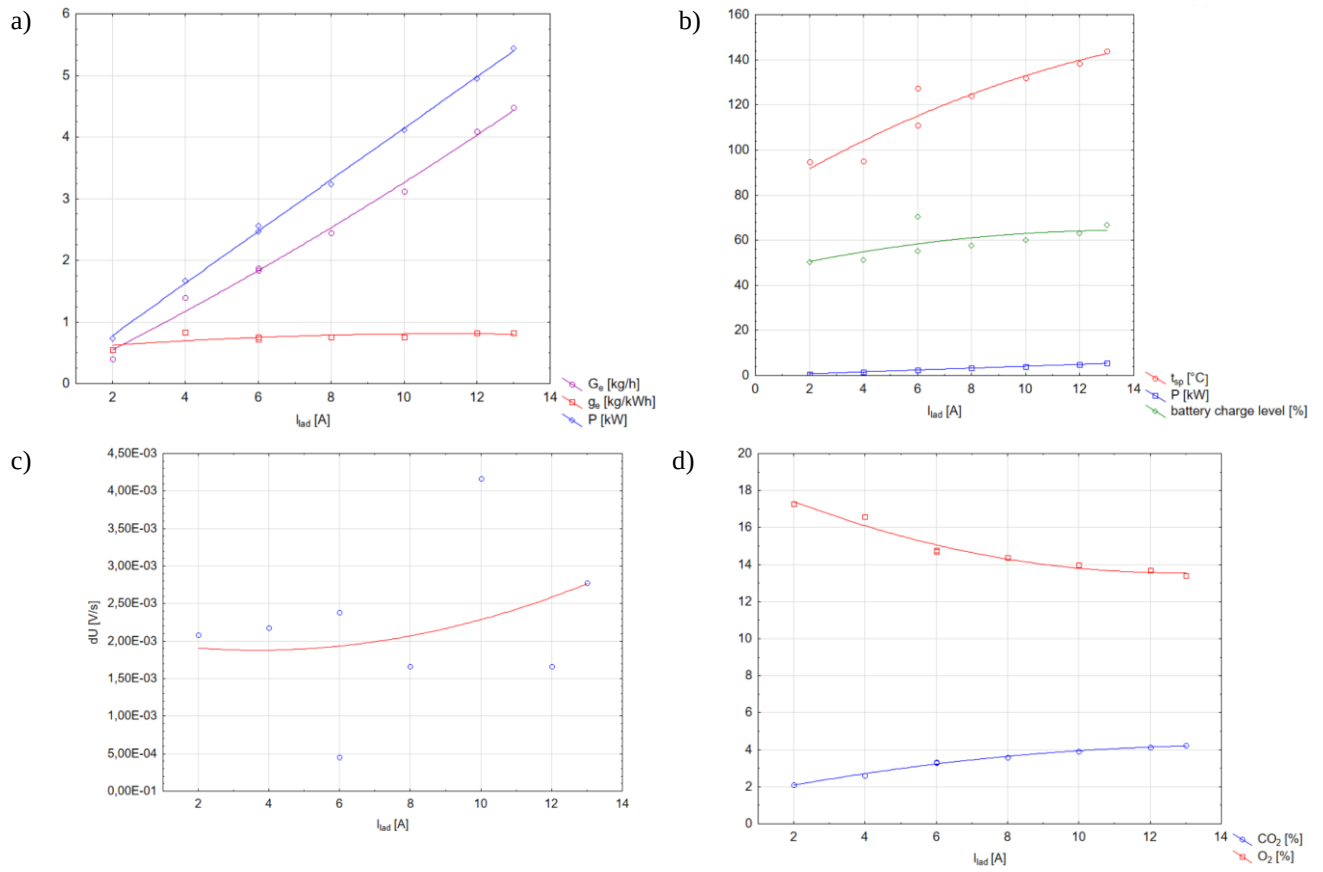

Fig. 15. Scatterplot of multiple variables against charging current I_{lad} a) G_e, g_e, P, b) t_{sp}, P, battery charge level, c) dU, d) CO_2, O_2

Analyzing the data obtained, it can be concluded that both battery currentI_{bat} and battery voltage drop dU show the highest correlations with the other measured quantities.

4.3. Analysis of the results for the load diagram

The analysis according to the load diagram was performed on the basis of the operating time balance of the motors presented in Chapter 3 (Fig. 10, Table 6).

Due to technical limitations of the test stand, measurements were not made for maximum values, i.e. n = 1400 rpm and M = 110 Nm. The tests (Fig. 14) according to the load balance are made for 60 minutes. The operating time for a given float mode was selected proportionally with the actual operating times of the drive.

Comparing the scatter plots for the test according to propeller characteristics (Fig. 13) with the scatter plots for the load diagram (Fig. 14), significant differences in the distribution of variables are apparent. This is due to the measurement times and the actual settings selected for the diagram in Fig. 14. Battery voltage drops over time for high current values are lower, which may allow the battery to run longer at a given load.

4.4. Analysis of results for battery charging

The analysis of the results for battery charging was performed based on the experimental plan shown in Table 7.

During start-up and preheating and cooling of the reformer, the test quantities were not measured due to the lack of measurement possibilities. Note the reformer's own operating time (i.e., the preheating process, which takes about 36 minutes, and the cooling time – 24 minutes). This represents about 33% of the device's operating time. The test results are shown in Fig. 15.

From the above scatter plots, it can be seen that an increase in the charging current affects the increase in the tested quantities. It should be noted that the magnitudes of the measured toxic compounds of the exhaust gas are close to zero. This has a positive effect on environmental protection, including a reduction in the emission of toxic compounds into the atmosphere.

5. Conclusion

The conducted studies, both empirical and model-based, prove that it is reasonable to use unconventional power sources for ship propulsion systems (equipped with fuel cells powered by hydrogen generated in a reformer), especially under specific operating conditions.

The main conclusions of the study are as follows:

1. The test object should be analyzed based on its specific load character.
2. The ship sails more than 50% of the task time in the very slow forward (BWN) mode. The battery voltage drop, for this mode, is the smallest at 1.263 mV/s for the test object.
3. As can be seen from the Pareto plots, speed and torque have the greatest influence on the quantities studied, while their linear and quadratic interactions are much less important.
4. Battery voltage drop is smallest for high loads and low speeds at the same time, or low loads and high speeds.

5. Both battery current I_{bat} and battery voltage drop dU show the highest correlations with the other measured quantities.
6. The magnitudes of the measured values of toxic compounds of exhaust gases are close to zero, and thus close to the values of the measuring resolution of TESTO 350. This is due to the nature of the combustion of methanol and has a beneficial effect on reducing their emission into the atmosphere.

In summary, the use of fuel cells can help improve air quality, reduce greenhouse gas emissions, and create a more efficient and sustainable energy system. However, it is worth noting that the implementation of this technology also requires consideration of aspects related to fuel (hydrogen) production and transportation. According to military assumptions, an undeniable benefit is the minimization of the physical fields of the vessel and its independence from the base (i.e., in the future, obtaining hydrogen from seawater electrolysis).

The promising results of the research will be continued. They will focus on developing a model for optimizing the selection of the battery buffer and placing it on the vessel so that the vessel's stability assumptions are maintained.

Nomenclature

AIS	automatic identification system	HPS	hybrid propulsion system
ANOVA	analysis of variance	HT	high temperature
DP	dynamic positioning	LT	low temperature
DV	dependent variable	PEMFC	polymer membrane fuel cell
FC	fuel cell	RMFC	reformed methanol fuel cell system
HESS	hybrid energy storage system		

Bibliography

[1] Acanfora M, Altosole M, Balsamo F, Micoli L, Campora U. Simulation modeling of a ship propulsion system in waves for control purposes. J Mar Sci Eng. 2022;10:36. https://doi.org/10.3390/jmse10010036

[2] Andersson M, Sundèn B. Technology review – solid oxide fuel cell. Report 2017:359, Energiforsk March 2017. www.energiforsk.se

[3] Barelli L, Bidini G, Gallorini F, Iantorno F, Pane N, Ottaviano PA, Trombetti L. Dynamic modeling of a hybrid propulsion system for tourist boat. Energies. 2018;11(10):2592. https://doi.org/10.3390/en11102592

[4] Buchanan F. PEM Fuel Cells: Theory, performance and applications. Nova Science Publisher. Hauppauge 2015.

[5] Dudek M, Lis B, Raźniak A, Krauz M, Kawalec M. Selected aspects of designing modular PEMFC stacks as power sources for unmanned aerial vehicles. Appl Sci. 2021;11(2):675. https://doi.org/10.3390/app11020675

[6] Dudek M, Raźniak A, Rosół M, Siwek T, Dudek P. Design, Development, and Performance of a 10 kW polymer exchange membrane fuel cell stack as part of a hybrid power source designed to supply a motor glider. Energies. 2020; 13(17):4393. https://doi.org/10.3390/en13174393

[7] Elammas T. Hydrogen fuel cells for marine applications: challenges and opportunities. International Journal of Research in Advanced Engineering and Technology. 2023; 9(1):38-43. www.allengineeringjournal.in

[8] Elkafas AG, Rivarolo M, Gadducci E, Magistri L, Massardo AF. Fuel cell systems for maritime: a review of research development, commercial products, applications, and perspectives. Processes. 2023;11(1):97. https://doi.org/10.3390/pr11010097

[9] Fakhreddine O, Gharbia Y, Derakhshandeh JF, Amer AM. Challenges and solutions of hydrogen fuel cells in transportation systems: a review and prospects. World Electr Veh J. 2023;14(6):156. https://doi.org/10.3390/wevj14060156

[10] Fu Z, Lu L, Zhang C, Xu Q, Zhang X, Gao Z et al. Fuel cell and hydrogen in maritime application: a review on aspects of technology, cost and regulations. Sustain Energy Tech Assessments. 2023;57:103181. https://doi.org/10.1016/j.seta.2023.103181.

[11] Fuel cell stack EH-51 15 kW. https://hyfindr.com/marketplace/components/fuel-cell-stacks/pem-stacks/fuel-cell-stack-eh-51-15-kw/

[12] Fuel cell systems for ships. https://new.abb.com/marine/systems-and-solutions/electric-solutions/fuel-cell (accessed on 5.02.2024).

[13] Habrat W, Żółkoś M., Świder J., Socha E. Forces modeling in a surface peripheral grinding process with the use of various design of experiment (DoE). Mechanik. 2018;91(10):929-931. https://doi.org/10.17814/mechanik.2018.10.165

[14] Hydrogen PEM fuel cell. https://hyfindr.com/pem-fuel-cell. Last update 15.02.2023. https://www.imo.org/en/OurWork/Environment/Pages/Default.aspx

[15] International Marine Organization. Regulation 13. http://www.marpoltraining.com/MMSKOREAN/MARPOL/Annex_VI

[16] International Maritime Organization. Regulations for the Prevention of Air Pollution from Ships: Annex VI MARPOL 73/78. 2005. Available online: https://www.epa.gov/sites/production/files/2016-09/documents/marpol-propose-revision-4-05.pdf

[17] Kniaziewicz T, Piaseczny L. Identification of marine internal combustion engine loads in terms of toxic exhaust emissions assessment (in Polish). Scientific Journals of AMW. 2011;187.

[18] Korzyński M. Experimental methodology. Planning, implementation and statistical processing of the results of technical experiments (in Polish). Publishing House of WNT. Warsaw 2017.

[19] Leo TJ, Durango JA, Navarro E. Exergy analysis of PEM fuel cells for marine applications. Energy. 2009;35(2):1164-1171. https://doi.org/10.1016/j.energy.2009.06.010

[20] Leśniewicz T. What is a planned experiment and can almost anything be improved with it?, https://sigmavalue.blog/planowany-eksperyment-doe/

[21] Li S, Gu C, Xu M, Li J, Zhao P, Cheng S. Optimal power system design and energy management for more electric aircrafts. J Power Sources. 2021;512:230473. https://doi.org/10.1016/j.jpowsour.2021.230473

[22] Li S, Gu C, Zhao P, Cheng S. A novel hybrid propulsion system configuration and power distribution strategy for light electric aircraft. Energy Convers Manage. 2021;238:114171. https://doi.org/10.1016/j.enconman.2021.114171
[23] Majka A, Muszyńska-Pałys J. Analysis of the performance of an aircraft powered by hybrid propulsion. Combustion Engines. 2023;193(2):45-51. https://doi.org/10.19206/CE-161107
[24] Marine Power: AKA Hybrid Propulsion. https://www.aka-group.com/marine-power/aka-hybrid-propulsion/
[25] Markowski J, Pielecha I. The potential of fuel cells as a transport drive source. IOP Conf Ser: Earth Environ Sci. 2019;214:012019. https://doi.org/10.1088/1755-1315/214/1/012019
[26] Meryem GS, Hüseyin TA. Advancements and current technologies on hydrogen fuel cell applications for marine vehicles. Int J Hydrogen Energ. 2022;47(45):19865-19875. https://doi.org/10.1016/j.ijhydene.2021.12.251
[27] MTU 8V2000 M72 Documentation.
[28] Nakano A, Shimazaki T, Sekiya M, Shiozawa H, Ohtsuka K, Aoyagi A et al. Research and development of liquid hydrogen (LH_2) temperature monitoring system for marine applications. Int J Hydrogen Energ. 2021;46(29):15649-15659. https://doi.org/10.1016/j.ijhydene.2021.02.052
[29] Online Statistics Handbook. Available online: https://www.statsoft.pl/textbook/stathome_stat.html
[30] User Manual H5-5000 V3 – 48 VDC.
[31] Van Hoecke L, Laffineur L, Campe R, Perreault P, Verbruggen SW, Lenaerts S. Challenges in the use of hydrogen for maritime applications. Energy Environ Sci. 2021;14:815-843. https://doi.org/10.1039/D0EE01545H
[32] Welaya YMA, El Gohary MM, Ammar NR. A comparison between fuel cells and other alternatives for marine electric power generation. Int J Nav Arch Ocean. 2011;3(2):141-149. https://doi.org/10.2478/IJNAOE-2013-0057
[33] Xing H, Stuart C, Spence S, Chen H. Fuel cell power systems for maritime applications: progress and perspectives. Sustainability. 2021;13(3):1213. https://doi.org/10.3390/su13031213
[34] Young Z, Shirong H, Xiaohui J, Yuntao Y, Mu X, Xi Y. Performance study on a large-scale proton exchange membrane fuel cell with cooling, Int J Hydrogen Energ. 2022;47:10381-10394. https://doi.org/10.1016/j.ijhydene.2022.01.122
[35] Yu W, Zhou P, Wang H. Evaluation on the energy efficiency and emissions reduction of a short-route hybrid sightseeing ship. Ocean Eng. 2018;162:34-42. https://doi.org/10.1016/j.oceaneng.2018.05.016
[36] Yuksel A. Engine emissions regulations for marine applications. Jun 28, 2021. https://www.cummins.com/pl/news/2021/06/28/engine-emission-regulations-marine-applications
[37] Zacharewicz M, Socik P, Wirkowski P, Zadrąg R, Bogdanowicz A. Evaluation of the impact of supplying a marine diesel engine with a mixture of diesel oil and n-butanol on its efficiency and emission of toxic compounds. Combustion Engines. 2023;195(4):40-47. https://doi.org/10.19206/CE-169484

Prof. Ryszard Zadrąg, DSc., DEng. – Faculty of Mechanical and Electrical Engineering, Polish Naval Academy, Poland.
e-mail: *r.zadrag@amw.gdynia.pl*

Prof. Marcin Zacharewicz, DSc., DEng. – Faculty of Mechanical and Electrical Engineering, Polish Naval Academy, Poland.
e-mail: *m.zacharewicz@amw.gdynia.pl*

Paweł Socik, MEng. – Faculty of Mechanical and Electrical Engineering, Polish Naval Academy, Poland.
e-mail: *p.socik@amw.gdynia.pl*

Artur Bogdanowicz, DEng. – Faculty of Mechanical and Electrical Engineering, Polish Naval Academy, Poland.
e-mail: *a.bogdanowicz@amw.gdynia.pl*

Prof. Tomasz Kniaziewicz, DSc., DEng. – Faculty of Mechanical and Electrical Engineering, Polish Naval Academy, Poland.
e-mail: *t.kniaziewicz@amw.gdynia.pl*

Paweł Wirkowski, DEng. – Faculty of Mechanical and Electrical Engineering, Polish Naval Academy, Poland.
e-mail: *p.wirkowski@amw.gdynia.pl*